HYPERPOLARIZED HELIUM-3 AND XENON-129 MAGNETIC RESONANCE IMAGING OF ELDERLY NEVER-SMOKERS AND EX-SMOKERS WITH CHRONIC OBSTRUCTIVE PULMONARY DISEASE

Miranda Kirby[1,2], Andrew Wheatley[1], Adam Farag[1], Alexei Ouriadov[1], Giles E Santyr[1], David G McCormack[3], and Grace Parraga[1,2]

[1]*Imaging Research Laboratories, Robarts Research Institute, London, ON, Canada,* [2]*Medical Biophysics, The University of Western Ontario, London, Ontario, Canada,* [3]*Division of Respirology, Department of Medicine, The University of Western Ontario*

Purpose: Hyperpolarized helium-3 (^{3}He) magnetic resonance imaging (MRI) provides a way to regionally quantify lung structural and functional measurements of chronic obstructive pulmonary disease (COPD). Unfortunately, the limited access to ^{3}He MRI and the high cost of ^{3}He gas has presented serious roadblocks for clinical translation. Another approach involves the use of hyperpolarized Xenon-129 (^{129}Xe) gas and this provides some distinct differences and advantages compared to ^{3}He MRI. The objective of this study was to directly and quantitatively compare hyperpolarized ^{3}He and hyperpolarized ^{129}Xe MRI, a less expensive and more readily available noble gas, in ex-smokers with COPD and age-matched never-smokers.

Materials and Methods

Subjects: All subjects provided written informed consent to a study protocol approved by the local research ethics board and Health Canada. Ex-smokers with a clinical diagnosis of COPD between the ages of 50-85 and a smoking history of ≥10 pack-years were enrolled. Elderly never-smokers were also enrolled who had no history of previous chronic or current respiratory disease. Spirometry and plethysmography were performed and the diffusing capacity of carbon monoxide (D_{LCO}) was measured according to the American Thoracic Society guidelines.

Image Acquisition: MRI was performed on a whole body 3.0 Tesla Discovery 750MR (General Electric Health Care, Milwaukee, WI) with broadband imaging capability as previously described[1]. ^{1}H images were acquired prior to ^{3}He and ^{129}Xe imaging with subjects scanned during a 1L breath-hold of ^{4}He/N_2 using the whole body RF coil and proton fast spoiled gradient-echo (16s total data acquisition, relaxation time (TR)/echo time (TE)/flip angle = 4.7 ms/1.2 ms/30°, field-of-view (FOV) = 40 x 40 cm, matrix 256 x 256, 14 slices, 15 mm slice thickness, 0 cm gap). For ^{3}He MRI, a polarizer system (HeliSpin™) was used to polarize ^{3}He gas. Hyperpolarized ^{3}He MRI coronal static ventilation images were acquired during breath-hold of a 1L ^{3}He/N_2 mixture (14s data acquisition, TR/TE /flip angle = 4.3 ms/1.4 ms/7°, bandwidth = 31.25, FOV = 40 × 40 cm, matrix 128 × 128, 14 slices, 15 mm slice thickness, 0 gap). For diffusion-weighted imaging, images were obtained using a fast gradient-echo method (FGRE). Two interleaved images (14s total data acquisition, TR/TE/flip angle = 7.6 ms/3.7 ms/8°, FOV = 40 x 40 cm, matrix 128 x 128, 7 slices, 30 mm slice thickness), with and without additional diffusion sensitization (G = 1.94 G/cm, rise and fall time = 0.5 ms, gradient duration = 0.46 ms, Δ = 1.46 ms, b = 1.6 s/cm^2), were acquired. For ^{129}Xe MRI a commercial turn-key polarizer model XeBox-E10 (Xemed LLC, New Hampshire, USA) was used. ^{129}Xe MRI coronal static ventilation images were acquired using a 3D FGRE during breath-hold of a 1L ^{129}Xe/^{4}He mixture (14s data acquisition, TR/TE/flip angle = 1.50 ms/6.7 ms/1.2°, bandwidth = 15.63, FOV = 40 × 40 cm, matrix 128 × 128, 14 slices, 15 mm slice thickness). For diffusion-weighted imaging, images were obtained using a 2D FGRE. Two interleaved images (16s total data acquisition, TR/TE/flip angle = 9.85 ms/11 ms/5°, bandwidth = 31.25, FOV = 40 x 40 cm, matrix 128 x 128, 7 slices, 30 mm slice thickness), with and without additional diffusion sensitization with b = 12 s/cm^2 (G = 2.90 G/cm, rise and fall time = 0.5 ms, gradient duration = 2.0 ms, Δ = 5 ms) and b = 20 s/cm^2 (G = 3.75 G/cm, rise and fall time = 0.5 ms, gradient duration = 2.0 ms, Δ = 5 ms), were acquired.

Image Analysis: ^{3}He and ^{129}Xe static ventilation images were segmented using semi-automated image segmentation/registration software as previously described[2]. Ventilation defect percent (VDP) was generated as the ventilation defect volume normalized to the thoracic cavity volume. ^{3}He and ^{129}Xe ADC maps were generated using in-house software. The image signal-to-noise ratio (SNR) for all images was also generated.

Statistical Analysis: A paired t-test was used to compare ^{3}He and ^{129}Xe SNR measurements and a two-way mixed design repeated measures analysis of variance was performed for comparison of ^{3}He and ^{129}Xe VDP measurements using SPSS 16.00. The relationship between ^{3}He and ^{129}Xe VDP and ADC measurements as well as pulmonary function measurements were determined using Pearson correlation coefficients (r) using GraphPad Prism version 4.00.

Results: For static ventilation images, ^{129}Xe VDP was statistically significantly higher than ^{3}He VDP for both COPD and age-matched never-smokers (p<.0001) and there was a significant interaction between the noble gas (^{129}Xe and ^{3}He) and group (COPD and age-matched never-smokers) (p=.02), indicating that there was a larger discrepancy between ^{129}Xe and ^{3}He VDP for the COPD subjects than the age-matched never-smokers (Figure 1). There was no significant correlation between the change in ^{3}He and ^{129}Xe SNR and the change in ^{3}He and ^{129}Xe VDP (r=.28, p=.26).

There was a strong and significant Pearson correlation between ^{3}He and ^{129}Xe VDP (r=.90, p<.0001) and ^{3}He and ^{129}Xe ADC (b=12s/cm^2: r=1.00, p<.0001; b=20 s/cm^2: r=.99, p<.0001). There was also a strong and significant Pearson correlation between ^{3}He VDP and $FEV_1\%_{pred}$ (r=-.84, p<.0001) and FEV_1/FVC (r=-.86, p<.0001) and between ^{129}Xe VDP and $FEV_1\%_{pred}$ (r=-.86, p<.0001) and FEV_1/FVC (r=-.93, p<.0001) for all subjects. ^{3}He ADC was significantly correlated with D_{LCO} (r=-.94, p<.0001) and ^{129}Xe ADC was also significantly correlated with D_{LCO} (b=12: r=-.95, p<.0001; b=20: r=-.91, p=.0002).

Conclusions: The finding that there were larger ventilation defects present in the ^{129}Xe as compared to the ^{3}He MR images, and that this difference was greater in COPD subjects, suggests that ^{129}Xe, a much larger and slowly diffusing gas in comparison to ^{3}He, may be more sensitive to the structural alternations that occur in the distal terminal and respiratory bronchioles where molecular movement by diffusion becomes the primary gas distribution mechanism. We have also demonstrated that the relationship between standard pulmonary function measurements is comparable between both noble gases, suggesting that ^{129}Xe MRI is feasible as an alternative to ^{3}He MRI with strong translational potential in COPD studies.

Table1. ^{3}He and ^{129}Xe MRI Measurements

Parameter	COPD (n=10)	Healthy Volunteer (n=8)
^{3}He MRI		
SV SNR (±SD)	32 (18)	26 (5)
$ADC_{b=1.6}$ SNR (±SD)	34 (22)	30 (7)
VDP % (±SD)	22 (8)	4 (2)
$ADC_{b=1.6}$ cm^2/s (±SD)	0.498 (0.116)*	0.244 (0.020)$^+$
^{129}Xe MRI		
SV SNR (±SD)	21 (11)	13 (6)
$ADC_{b=12}$ SNR (±SD)	18 (13)*	8 (1)$^{++}$
$ADC_{b=20}$ SNR (±SD)	22 (20)**	14 (10)‡
VDP % (±SD)	34 (11)	9 (5)
$ADC_{b=12}$ cm^2/s (±SD)	0.081 (0.014)*	0.052 (0.002)$^{++}$
$ADC_{b=20}$ cm^2/s (±SD)	0.068 (0.013)**	0.044 (0.003)‡

*n=9, **n=8, $^+$n=6, $^{++}$n=3, ‡n=4

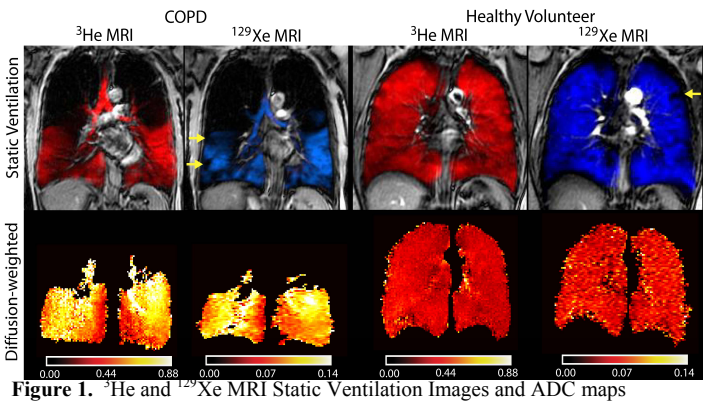

Figure 1. ^{3}He and ^{129}Xe MRI Static Ventilation Images and ADC maps

References

1. Parraga, G. *et al. Invest Radiol.* (2007).
2. Kirby, M. *et al. Acad Radiol.* (2011).